

Supporting Information

**Rational Design of Polyaniline/MnO₂/Carbon Cloth Ternary Hybrids
as Electrodes for Supercapacitors**

Xin Zhao¹, Chaoyi Chen¹, Zilong Huang¹, Lei Jin¹, Junxian Zhang¹, Yingzhi Li¹, Lili Zhang^{2*}, and Qinghua Zhang^{1*}

¹*College of Material Science & Engineering, State Key Laboratory for Modification of Chemical Fibers and Polymer Materials, Donghua University, Shanghai 201620, China*

²*Institute of Chemical and Engineering Sciences, A*STAR, 1 Pesek Road, Jurong Island 627833, Singapore*

*Corresponding author. Email: zhang_lili@ices.a-star.edu.sg, qhzhang@dhu.edu.cn

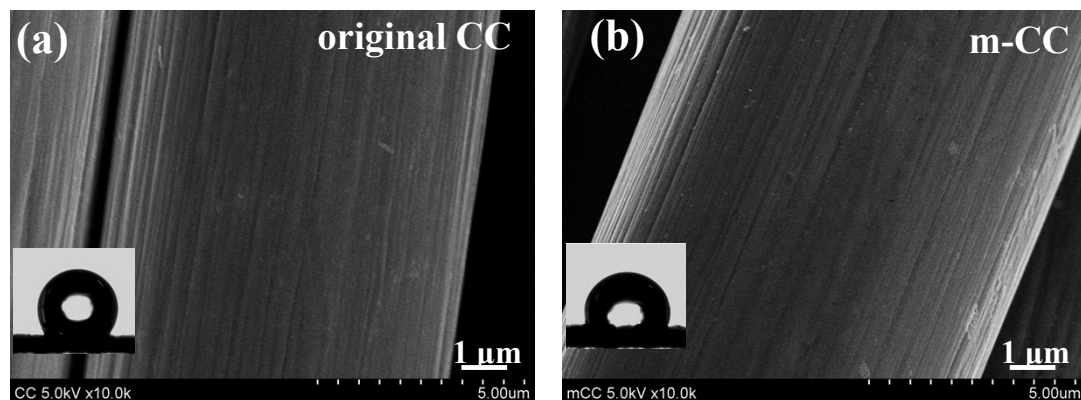


Figure S1. SEM images of original CC and m-CC and their hydrophilic tests (inset shows the contact angle).

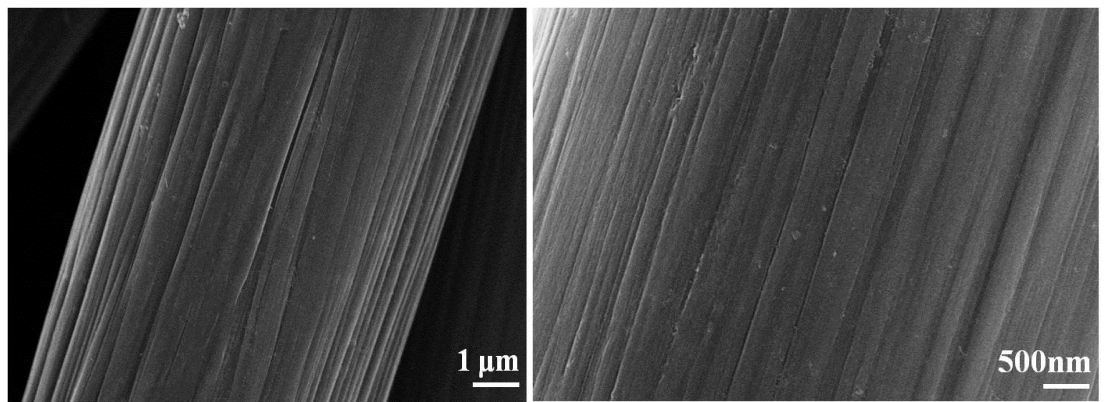


Figure S2. SEM images of m-CC after being etched in 1 M H_2SO_4 .

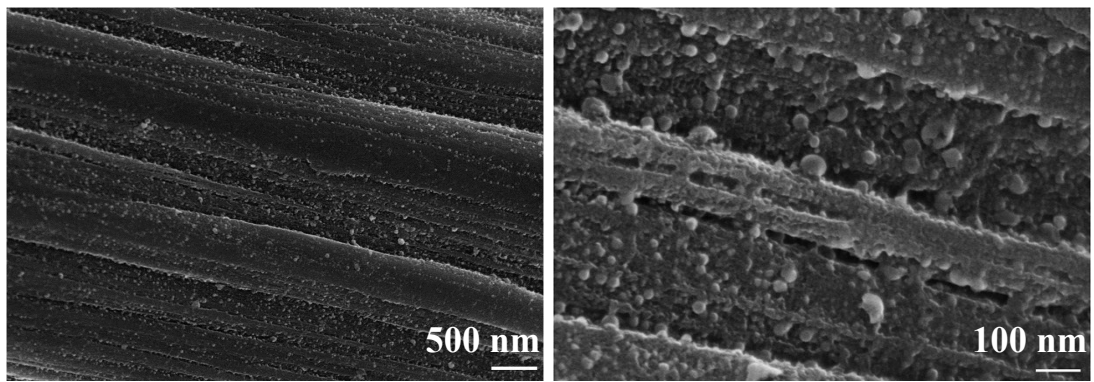


Figure S3. SEM images of $\text{MnO}_2@\text{m-CC}$ after being etched by 1 M H_2SO_4 .

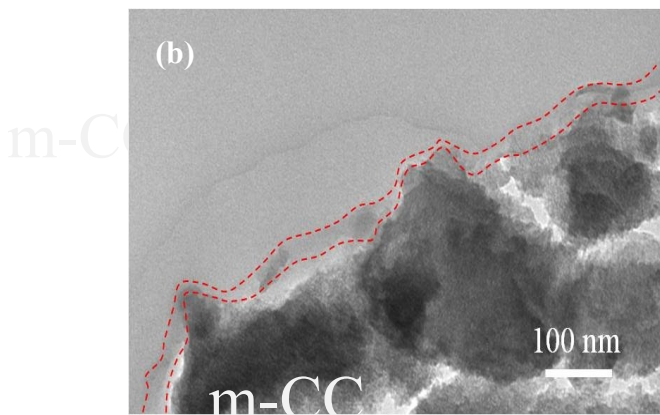


Figure S4. TEM images of (a) MnO₂@PANI@m-CC and (b) PANI@MnO₂@m-CC

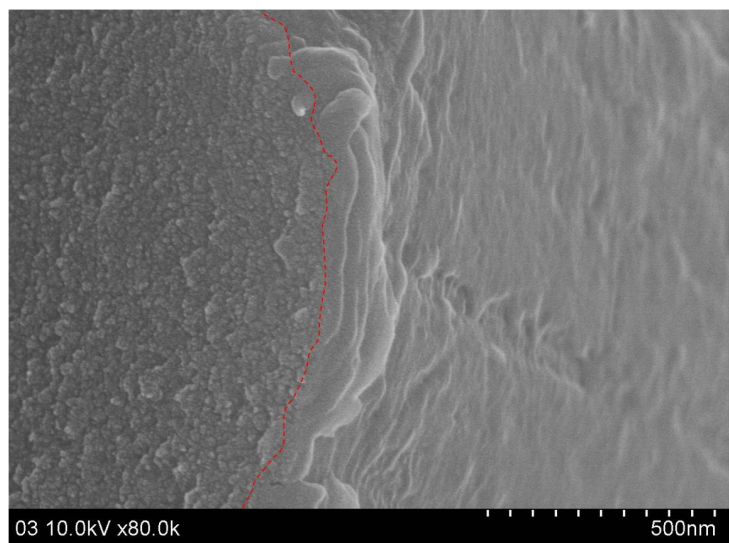


Figure S5. SEM image of the cross-section part of PANI@MnO₂@m-CC

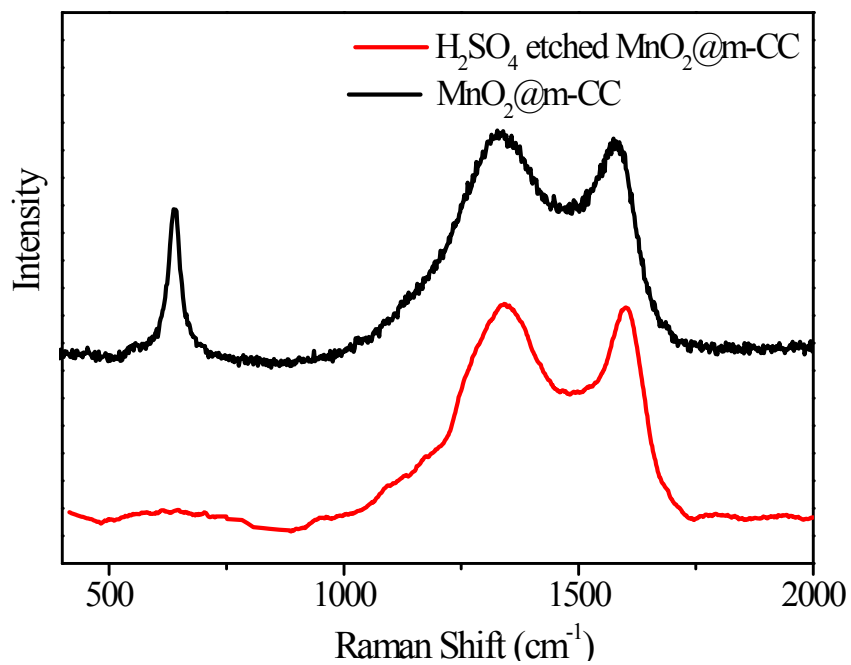


Figure S6. Raman spectra of H_2SO_4 etched $\text{MnO}_2@\text{m-CC}$ and original $\text{MnO}_2@\text{m-CC}$

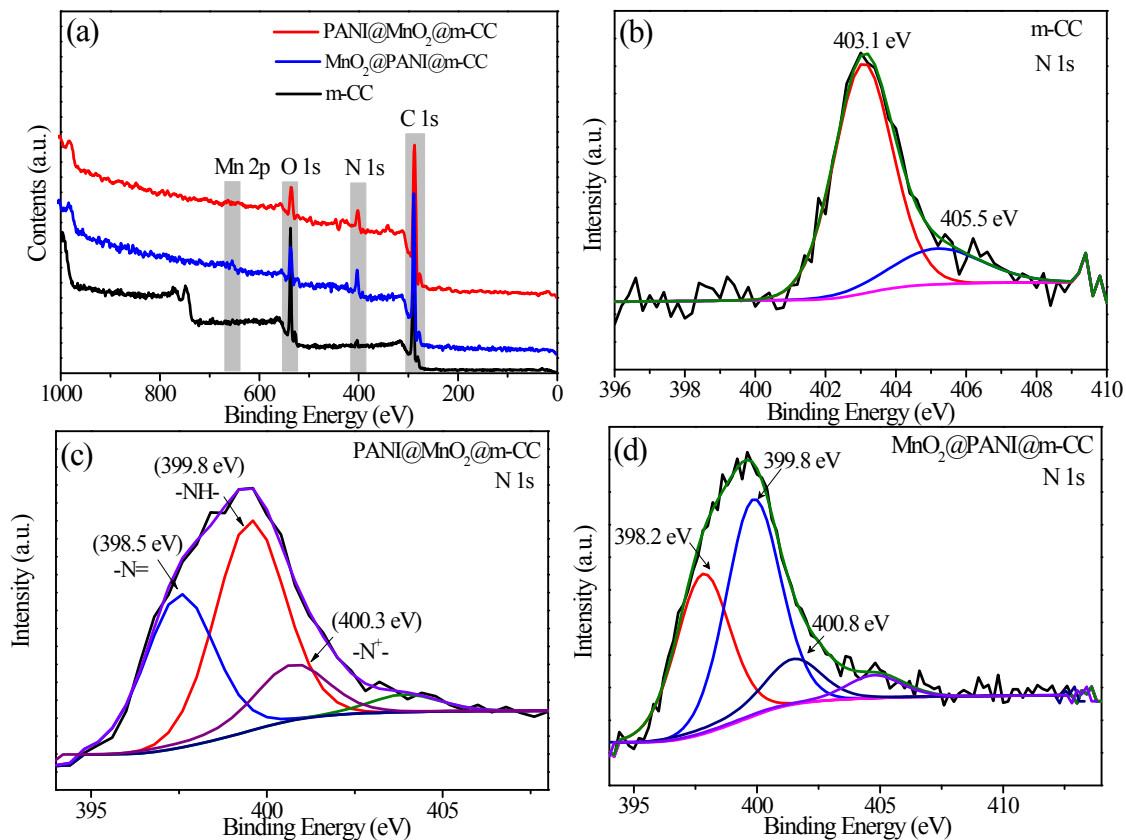


Figure S7. (a) Survey XPS spectrum of m-CC, PANI@MnO₂@m-CC, MnO₂@PANI@m-CC and N 1s spectra of (b) m-CC, (c) PANI@MnO₂@m-CC and (d) MnO₂@PANI@m-CC

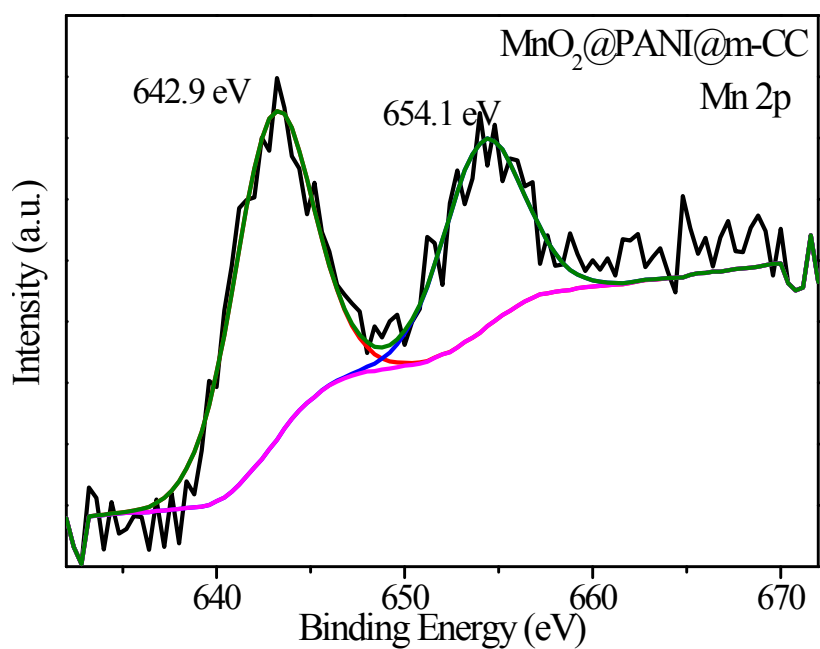


Figure S8. Mn 2p spectra for $\text{MnO}_2@\text{PANI}@m\text{-CC}$

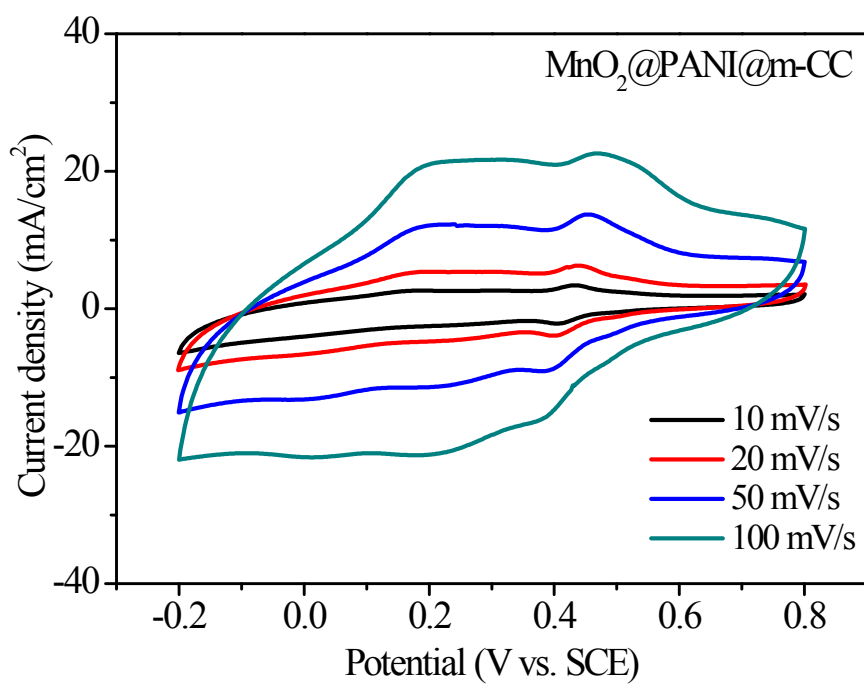


Figure S9. CV curves of $\text{MnO}_2@\text{PANI}@m\text{-CC}$ at various scan rates.

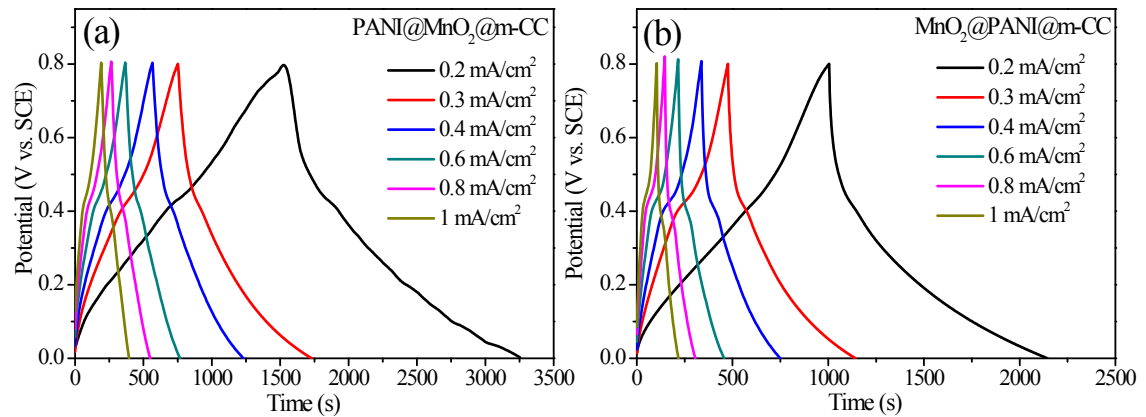


Figure S10. Galvanostatic charge/discharge curves of (a) $\text{PANI}@\text{MnO}_2@\text{m-CC}$ and (b) $\text{MnO}_2@\text{PANI}@ \text{m-CC}$ at different current densities

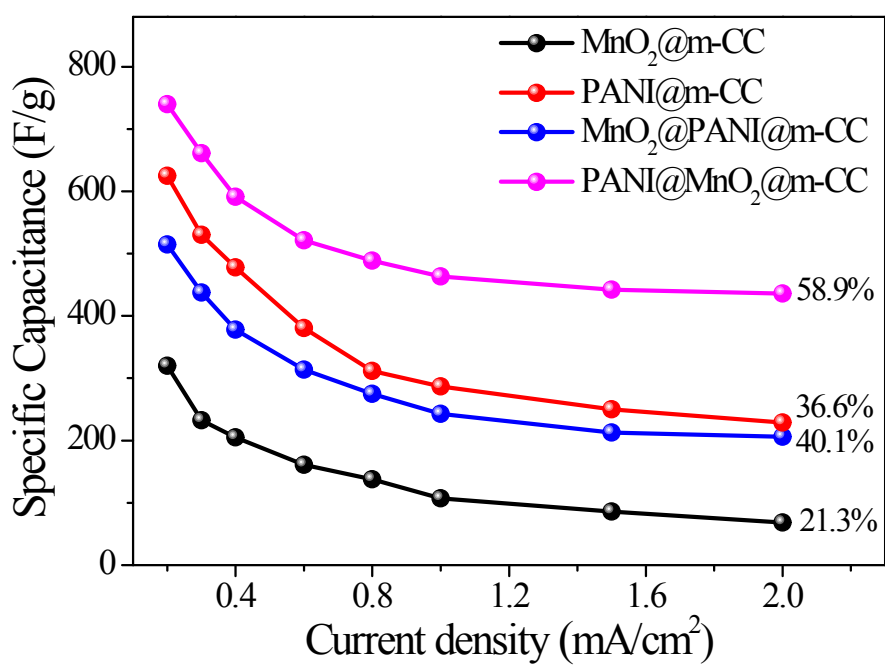


Figure S11. Gravimetric specific capacitance *vs.* current densities of as-prepared samples.

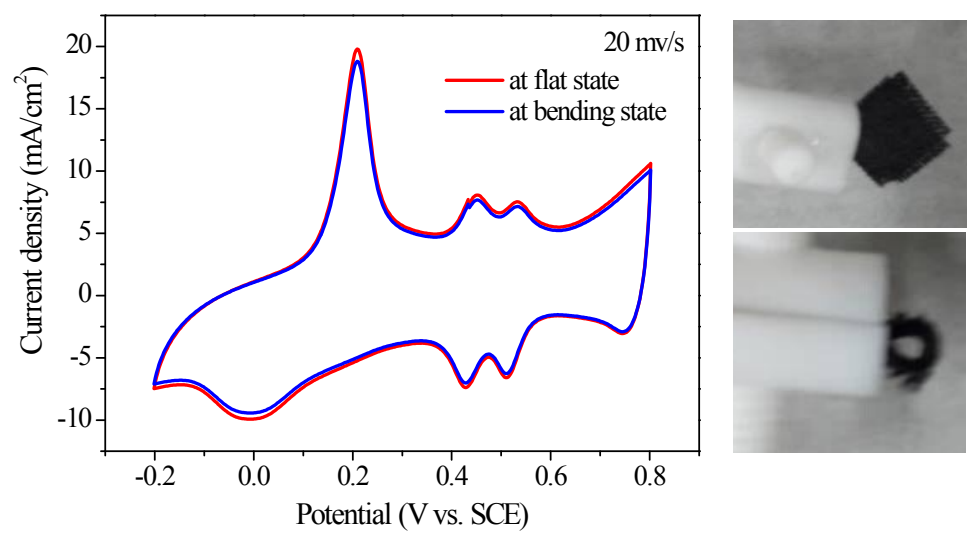


Figure S12. CV curves at 20 mV/s of PANI@MnO₂@m-CC electrode at flat and bending state

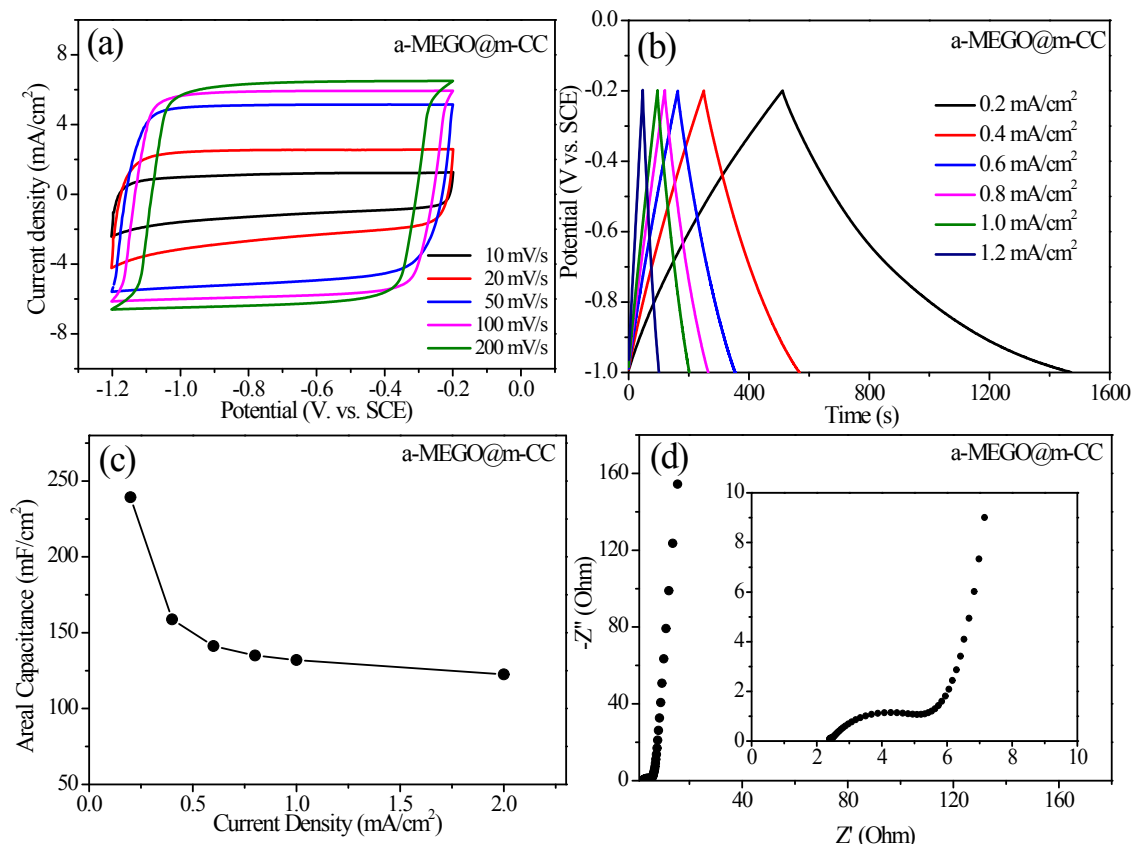


Figure S13. Three-electrode electrochemical measurements of a-MEGO@m-CC: (a) CV curves at various scan rates, (b) Galvanostatic charge/discharge curves at different current densities, (c) plot of areal capacitance vs. current density and (d) Nyquist plot from EIS measurement.

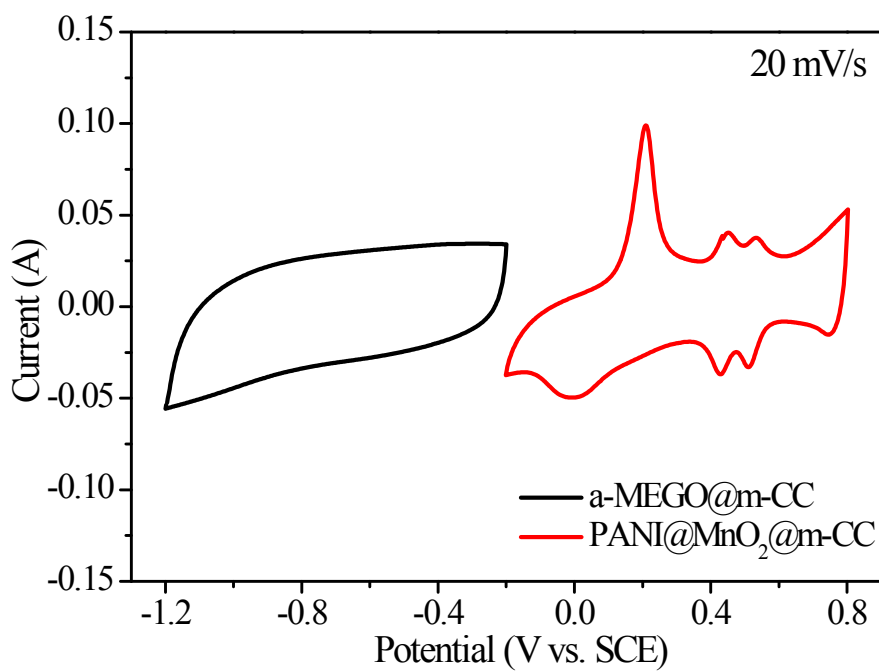


Figure S14. Comparison of the CV curves of a-MEGO@m-CC and PANI@MnO₂@m-CC at different potential window in three electrode systems.

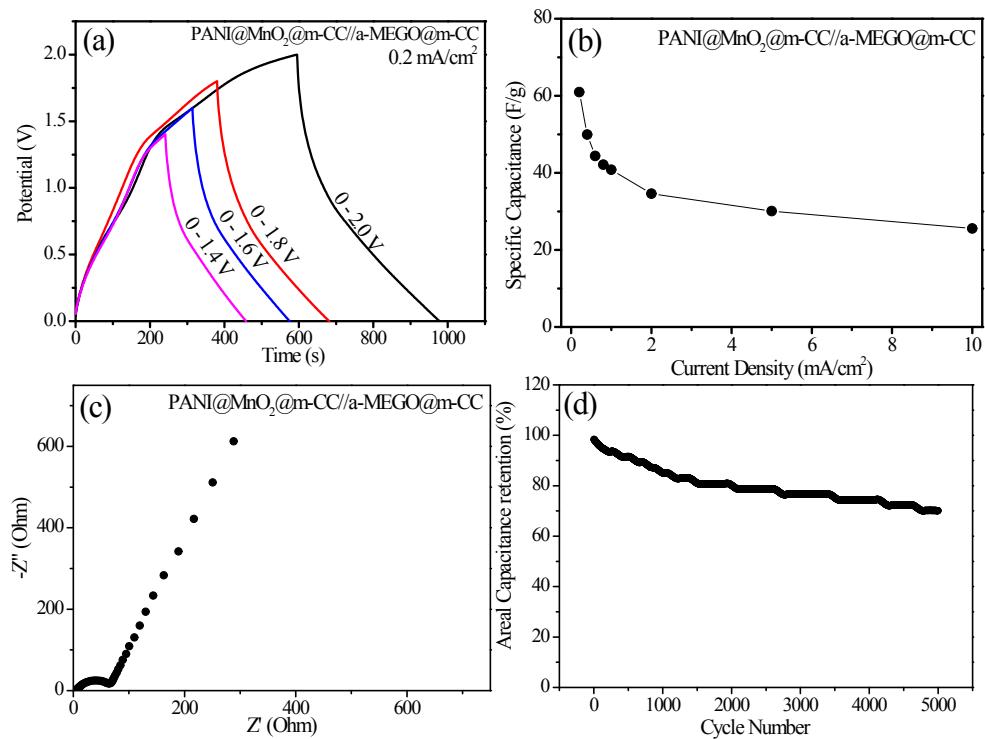


Figure S15. (a) Galvanostatic charge/discharge curves at a current density of 0.2 mA/cm² with different potential windows, (b) plots of gravimetric specific capacitance vs. current density, (c) Nyquist plots and (d) cycling stability curves of assembled PANI@MnO₂@m-CC//a-MEGO@m-CC ASC device.

Table S1. The total mass of each samples obtained in our work.

Samples ($1 \times 1 \text{ cm}^2$)	Mass (mg)							
m-CC	9.95	9.51	9.48	9.63	9.87	10.02	9.62	9.90
MnO ₂ @m-CC	10.15	9.73	9.70	9.84	-	-	-	-
PANI@m-CC	-	-	-	-	10.22	10.40	9.98	10.25
PANI@MnO ₂ @m-CC	10.50	10.11	10.05	10.21	-	-	-	-
MnO ₂ @PANI@m-CC	-	-	-	-	10.43	10.63	10.20	10.47

Table S2. Calculated areal and gravimetric specific capacitance of a-MEGO@m-CC and PANI@MnO₂@m-CC at different current densities in a three electrode system.

Samples	Capacitance	Current density (mA/cm ²)					
		0.2	0.4	0.6	0.8	1.0	2.0
a-MEGO@m-CC (0.97 mg/cm ²)	C_{areal} (mF/cm ²)	239.3	158.8	141.2	140	132	132.5
	C_{m} (F/g)	246.6	163.7	145.6	144.4	136.1	136.6
PANI@MnO ₂ @m- CC (0.57 mg/cm ²)	C_{areal} (mF/cm ²)	421.6	337.1	297	278.6	264.1	251.3
	C_{m} (F/g)	739.6	591.4	521.1	488.8	463.3	440.9